Bioconjugate Chemistry

Article

pubs.acs.org/bc

Triazine-Based Tool Box for Developing Peptidic PET Imaging Probes: Syntheses, Microfluidic Radiolabeling, and Structure–Activity Evaluation

Hairong Li,[†] Haiying Zhou,[†] Stephanie Krieger,[‡] Jesse J. Parry,[‡] Joseph J. Whittenberg,[§] Amit V. Desai,[§] Buck E. Rogers,[‡] Paul J. A. Kenis,[§] and David E. Reichert*,[†]

[†]Radiological Sciences Division, Mallinckrodt Institute of Radiology, Washington University School of Medicine, 510 South Kingshighway Boulevard, St. Louis, Missouri 63110, United States

[‡]Department of Radiation Oncology, Washington University School of Medicine, 4511 Forest Park Boulevard, St. Louis, Missouri 63108, United States

[§]Department of Chemical & Biomolecular Engineering, University of Illinois at Urbana–Champaign, Urbana, Illinois 61801, United States

Supporting Information

ABSTRACT: This study was aimed at developing a triazine-based modular platform for targeted PET imaging. We synthesized mono- or bis-cyclo(RGDfK) linked triazine-based conjugates specifically targeting integrin $\alpha_v\beta_3$ receptors. The core molecules could be easily linked to targeting peptide and radiolabeled bifunctional chelator. The spacer core molecule was synthesized in 2 or 3 steps in 64–80% yield, and the following conjugation reactions with cyclo(RGDfK) peptide or bifunctional chelator were accomplished using "click" chemistry or amidation reactions. The DOTA-TZ-Bis-cyclo(RGDfK) **13** conjugate was radiolabeled successfully with $^{64}Cu(OAc)_2$ using a microfluidic method, resulting in higher specific activity with above 95% labeling yields compared to conventional radiolabeling (SA ca. 850 vs 600 Ci/mmol). The dimeric cyclo(RGDfK) peptide was found to display significant bivalency effect using I^{125}-*Echistatin* binding assay with IC_{50} value as 178.5 ± 57.1 nM, which displayed a 3.6-fold enhancement of binding affinity compared to DOTA-TZ-cyclo(RGDfK) **14** conjugate on U87MG human glioblastoma cell. Biodistribution of all four conjugates in female athymic nude mice were evaluated. DOTA-"Click"-cyclo(RGDfK) **15** had the highest tumor uptake among these four at 4 h p.i. with 1.90 ± 0.65%ID/g, while there was no clear bivalency effect for DOTA-TZ-BisRGD *in vivo*, which needs further experiments to address the unexpected questions.

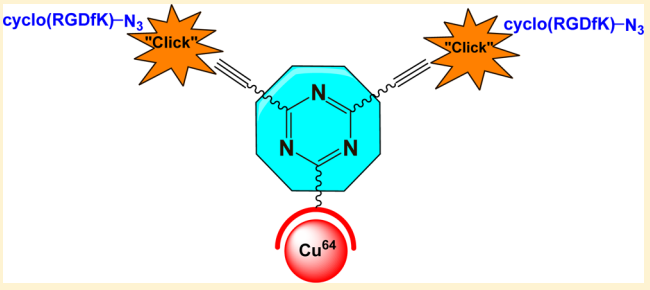

INTRODUCTION

The integrin $\alpha_v\beta_3$ receptor has been widely studied due to its major role in tumor angiogenesis and metastasis, and osteoclast mediated bone resorption.[1] DOTA conjugated cyclic arginine-glycine-aspartic acid (RGD) peptides have been synthesized as molecular imaging agents of integrin $\alpha_v\beta_3$ expression,[2] and several research groups have reported multimeric cyclo-(RGDfK) imaging probes with higher tumor uptake and improved pharmacokinetic profiles.[3] "Click chemistry" utilizing the reactions of organic azides and terminal alkynes to form 1,2,3-triazoles by Huisgen 1,3-dipolar cycloaddition reactions catalyzed by Cu (I)[4] provides an attractive route for the preparation of radiopharmaceuticals, especially those utilizing biomolecules due to its bioorthogonal nature. There are quite a few examples demonstrating the application of "click chemistry" in radiopharmaceuticals, e.g., ^{18}F-labeled RGD peptides,[5] ^{111}In-DOTA-conjugated octreotide,[6] ^{99m}Tc-galacto-RGD dimer peptide,[7] or ^{64}Cu(^{68}Ga)-DOTA-conjugated RGD peptides,[8] and so forth. We have developed a multifunctional triazine-based scaffold as a toolkit for producing targeted positron emission tomography (PET) imaging probes with a variety of choices for receptor targeting ligands and different nuclear or optical imaging groups. The main goal of this study was to demonstrate the synthetic feasibility of a triazine-based modular platform, in which the spacer core molecule could be conveniently linked to targeting groups (multimeric or monomeric) and bifunctional chelator labeled with radiometal using either "click chemistry" or standard amidation reactions from an activated NHS ester. The "mix and match" concept allows the rapid synthesis of preclinical drug candidates for PET or optical imaging.

Herein, we successfully prepared the triazine-based spacer core, in a stepwise manner under temperature-controlled or microwave conditions with high synthetic yields. We selected

Received: January 24, 2014
Revised: March 18, 2014
Published: March 24, 2014

Scheme 1. Synthesis of Triazine Spacers 8 and 9

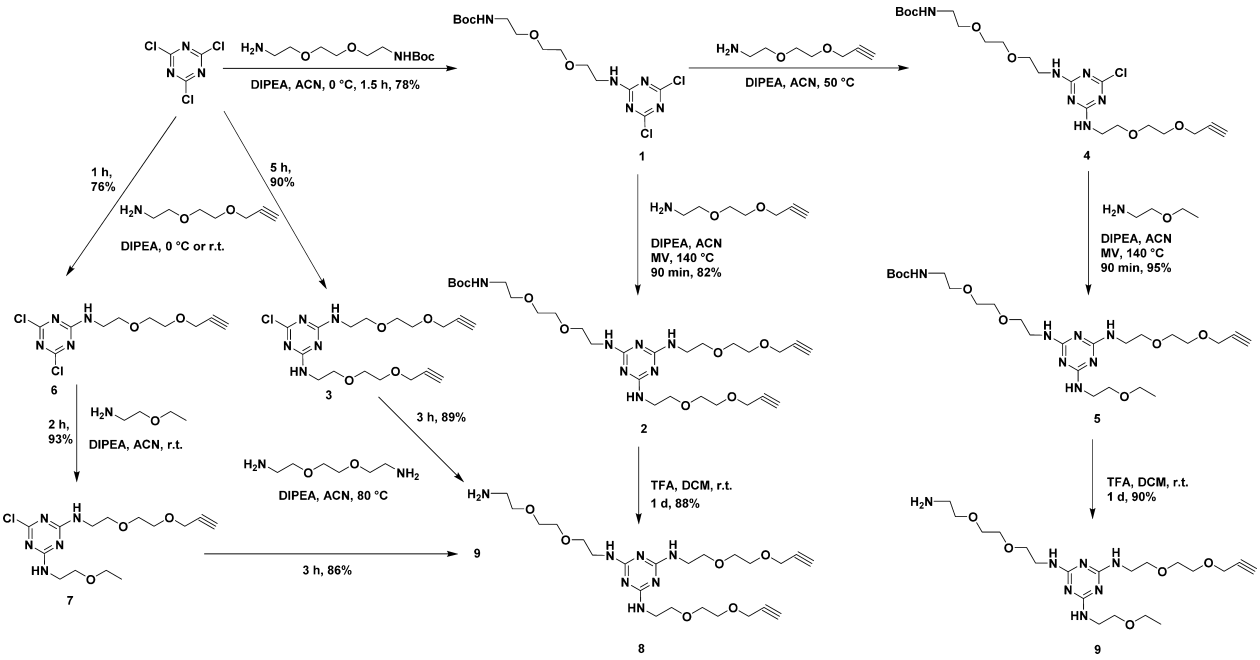

Scheme 2. Synthesis of DOTA Conjugated cyclo(RGDfK) Peptides 13−15

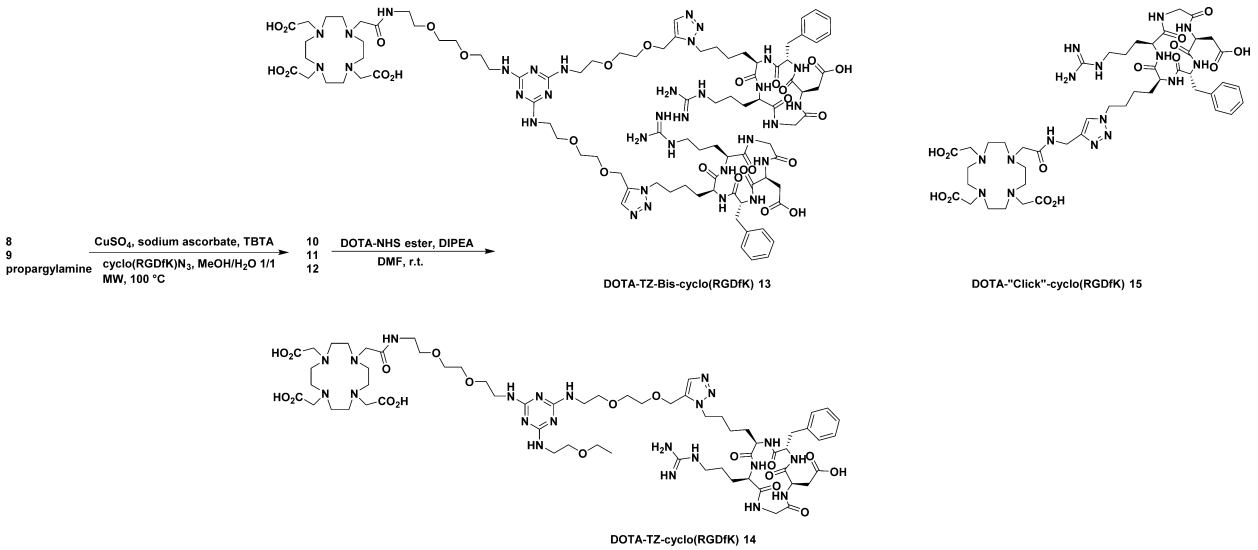

the cyclo(RGDfK) peptide for targeting integrin $\alpha_v\beta_3$ receptors as a proof-of-principle demonstration. Radiolabeling with copper-64 was achieved on microfluidic chips with repeatable excellent radiolabeling yields and high specific activity. We also evaluated *in vitro* receptor binding affinity and *in vivo* biodistribution.

RESULTS AND DISCUSSION

Chemistry. It has been recognized that cyclo(-Arg-Gly-Asp-D-Phe-Val-) is a targeting peptide for integrin $\alpha_v\beta_3$ receptors and inhibits tumor angiogenesis.[9] It was reported that lysine (K) or glutamic acid (E) could replace the valine (V) residue at the fifth position without affecting the integrin binding affinity.[9a,10] Since the amino group on lysine amino acid could be easily modified, we synthesized azido-functionalized cyclo(RGDfK) peptide starting from Fmoc-Gly-2Cl-Trt resin using standard Fmoc solid-phase peptide synthesis chemistry. Fmoc-Arg(Pbf)-OH, Fmoc-Lys(N_3)-OH, Fmoc-(D)Phe-OH, and Fmoc-Asp(O^{t}Bu)-OH (3 equiv for each) were coupled to the resin sequentially by using HBTU/DIPEA coupling agents after deprotection of the Fmoc group from the C-terminus on the resin using piperidine. After the synthesis of the linear peptide on the peptide synthesizer, the desired cyclic peptide was synthesized by following the cleavage, cyclization, and deprotection steps developed by Dai et al.[11] The overall yield from the starting Fmoc-Gly-2Cl-Trt resin was 31% yield after purification by reverse-phase high performance liquid chromatography.

The use of a triazine molecule as a molecular core has been reported for a dendrimer construct for viral transfection,[12] drug delivery,[13] antibody targeting,[14] or gadolinium based MRI agents.[15] Cyanuric chloride was used as a core molecule for sequential modifications using reported temperature controlled methods.[16] There are two routes to synthesize the

dx.doi.org/10.1021/bc500034n | *Bioconjugate Chem.* 2014, 25, 761−772

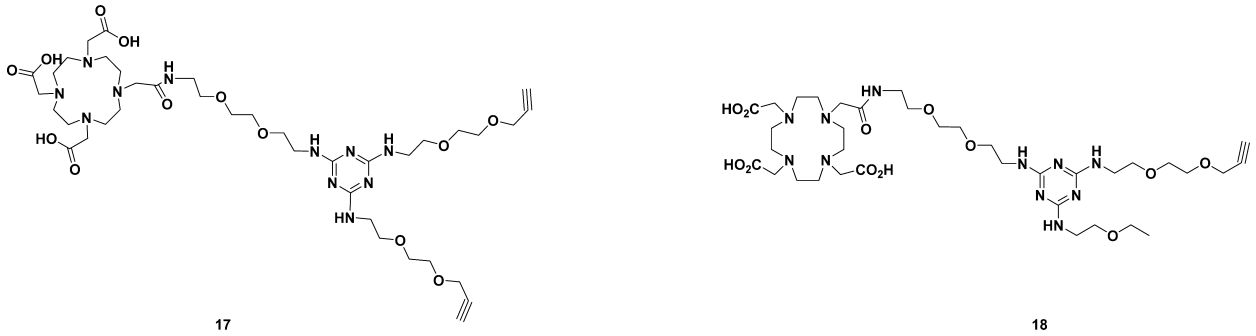

Figure 1. Chemical structures of DOTA conjugated triazine spacers **17** and **18**.

trisubstituted triazine spacers (**8**, **9**) (Scheme 1). The cyanuric chloride was first reacted with *tert*-butyl-(2-(2-(2-aminoethoxy)ethoxy)ethyl)carbamate linker (SI) at 0 °C to afford intermediate spacer **1** in the presence of DIPEA in 78% yield. Spacer **1** then reacted with 2-(2-(prop-2-ynyloxy)-ethoxy)ethan-1-amine (SI) under microwave irradiation at 140 °C to afford bis-PEG-alkyne-substituted triazine spacer **2** in 82% yield. Mono-PEG-alkyne-substituted triazine spacer **4** could be afforded with second substitution of 2-(2-(prop-2-ynyloxy)ethoxy)ethan-1-amine linker by heating at 55 °C in 93% yield. Spacer **4** then reacted with 2-ethoxylethylamine to afford spacer **5** under microwave irradiation at 140 °C in 95% yield. The *t*-butyloxycarbonyl (BOC) protecting groups on both spacers **2** and **5** linker ends were removed by trifluoroacetic acid/dichloromethane (v/v:1/1) solution at room temperature to afford pure amino-ended PEG linker substituted triazine spacer which were functionalized with one or two acetylene moieties (**8**, **9**) in ca. 90% yield after HPLC purification. An alternate route to synthesize spacer **8**, which avoids the deprotection step and tedious HPLC purification, starts with the reaction of cyanuric trichloride and 2-(2-(prop-2-yn-1-yloxy)ethoxy)ethan-1-amine (2.6 equiv) in the presence of DIPEA (2 equiv) to afford the stable monochloro-bis-PEG-acetylene substituted triazine spacer **3** in 90% yield. Spacer **3** reacts with large excess of 2,2′-(ethylenedioxy)bis(ethylamine) (40 equiv) and DIPEA (20 equiv) in anhydrous acetonitrile to afford pure triazine spacer **8** in 89% yield after flash chromatography on silica gel. A similar method was applied to synthesize triazine spacer **9** containing one acetylene moiety in three steps. In summary, the construction of triazine spacer containing acetylene and amino functionalities could be achieved in three or four steps using amino-BOC protected PEG linker in 56−69% total yield. Avoiding the use of a protection−deprotection strategy, the total synthesis of the spacer molecule could be accomplished in two or three steps of 80% total yield for spacer **8** containing two acetylene moieties, or 64% total yield for spacer **9** containing one acetylene moiety.

Triazine spacers **8** and **9** reacted with 2.7 or 1.3 equiv azido-functionalized cyclo(RGDfK) peptide using "click chemistry" in the presence of TBTA-Cu (I) catalyst complex (13%) at 100 °C under microwave irradiation for 40−60 min (Scheme 2). The bis or monocyclo(RGDfK) conjugated triazine spacers **10** and **11** were obtained in 90% and 79% yield after HPLC purification. Different solvent systems for the reaction were attempted. The protic solvent combination methanol:water (1:1) was found to have the best yield for the "click" reaction under microwave irradiation. The peptide conjugates **10** and **11** reacted with DOTA-NHS ester in anhydrous DMF in the presence of 6 equiv DIPEA to afford the final DOTA conjugated bis- or mono- cyclo(RGDfK) peptides in ca. 45% yield after purification. The DOTA-cyclo(RGDfK) standard peptide[17] was synthesized via common amidation reaction from DOTA-NHS ester and amino-functionalized cyclo(RGDfK) peptide (Supporting Information). DOTA-"Click"-cyclo-(RGDfK) **15** peptide was synthesized from "click" reaction between azido modified cyclo(RGDfK) and propargylamine, which was followed by amidation reaction with DOTA-NHS ester.

The "click chemistry" between the acetylene group(s) of the core molecules and cyclo(RGDfK)-N_3 was challenging. First, we synthesized DOTA-conjugated triazine precursors **17** and **18** (Figure 1) through amidation reaction from activated DOTA-NHS ester and triazine spacer **8** and **9**. Then, we were unable to obtain the "click" product from free DOTA-conjugated triazine and cyclo(RGDfK)-N_3 using TBTA-Cu (I) catalyst under various reaction conditions such as microwave irradiation or heating at high temperature (e.g., 100 °C) overnight. Subsequent investigation determined that TBTA-Cu (I) was not stable in the presence of free DOTA, which would chelate copper as a DOTA-Cu (II) complex. Starting from chelated DOTA-Cu (II)-conjugated triazine spacer, the "click" reaction with cyclo(RGDfK)-N_3 peptide was complete in 1 h under microwave irradiation at 100 °C with 100% conversion yield, while under conventional heating at 80 °C for 18 h we only obtained 50% conversion yield (Supporting Information). Starting from the chelated DOTA-Gd (III)-conjugated triazine spacer, the product could be obtained under microwave irradiation at 100 °C for 1 h with ca. 30% conversion yield. The chelated Cu (II) would decrease the Cu (II)−Cu (I) redox couple efficiency to generate active Cu (I) catalyst.[8a] As a result, there is insufficient Cu (I) to serve as catalyst for the click reaction.

These results implied that free DOTA was more likely to access copper to form DOTA-Cu (II) complex than TBTA ligand (TBTA-Cu (I) complex). To further validate the process, we performed a DOTA-TBTA competitive chelation study using carrier-added ^{64}Cu. Equal moles DOTA-tetra-carboxylic acid and TBTA-^{64}Cu (carrier added) were mixed for 15 min at ambient temperature. We observed that DOTA-^{64}Cu (II) was produced from TBTA-^{64}Cu (I) in 100% yield after 15 min, as determined by radio-TLC (Supporting Information). Since DOTA could quench the copper catalyst during the "click" reaction and the chelated DOTA-Cu (II) would also decrease the radiolabeling yield in a later step, the synthesis of cyclo(RGDfK)-"click"-triazine process was performed prior to the DOTA conjugation reaction via amidation. The "click" reaction could be catalyzed with 13% copper(I)-TBTA complex under microwave irradiation at 100 °C for 40 min to afford

dx.doi.org/10.1021/bc500034n | *Bioconjugate Chem.* 2014, 25, 761−772

Table 1. Microfluidic (MF) and Conventional (CV) Radiolabeling of Peptide 13 with $^{64}Cu(OAc)_2$

radiolabeling method	temp (°C)	reaction scale/ [ligand] (μM)	reaction volume (μL)	total ligand mass (μg)	experimental L/M ratio	time (min)	HPLC labeling yield (%)	calculated SA (Ci/ mmol)
MF	37	4.5	52.6	0.5	2.1	10	97.4 ± 2	867.1 ± 88
MF	37	4.6	52.6	0.5	7.5	10	97.8 ± 0.8	850.9 ± 84.9
CV	90	9.1	192	3.7	62.3	30	99.0	535.5

NH_2-TZ-cyclo(RGDfK) **11** in 79% yield. NH_2-TZ-Bis-cyclo-(RGDfK) **10** containing two cyclo(RGDfK) peptides was easily synthesized under the same microwave conditions for 60 min in 90% yield. When using conventional heating conditions, extended reaction time was needed. Only monocyclo(RGDfK) conjugated triazine spacer was observed from MALDI-TOF spectroscopy after the reaction of spacer **8** and cyclo(RGDfK)-N_3 peptide under conventional heating at 80 °C for 18 h. No bis-cyclo(RGDfK)-conjugated triazine was observed even after 42 h in the presence of 25% Cu (I)-TBTA catalyst complex. Thus, microwave heating was found to be the preferred method to synthesize the "click" peptide product, especially the bis-peptide conjugated compound. The "click" reaction could be monitored by MALDI-TOF mass spectroscopy at 1084.6 m/z (**11**, $[M]^+$) or 1768.9 (**10**, $[M+H]^+$). Both the "click" product and the DOTA conjugate could be purified with HPLC on reverse phase (C18) column in reasonable yields.

Conventional and Microfluidic Radiolabeling on Chip. The microfluidic radiolabeling of DOTA-TZ-Bis-cyclo-(RGDfK) **13** containing two cyclo(RGDfK) motifs was achieved with ligand to metal ratios of 2−7 for each reaction (Table 1). The ligand concentration was 4.5 μM and total mass of the ligand was 0.5 μg. The radiolabeling process was performed on chip at 37 °C for 10 min. The radiolabeling yield was >97% evaluated by radio-HPLC. The specific activity ranged from 850.9 ± 84.9 to 867.1 ± 88 Ci/mmol (n = 4 or 5). The conventional radiolabeling was performed under normally reported condition.[2c,d] The reaction scale was about 3.7 μg peptide per mCi ^{64}Cu in 200 μL buffer solution (NaOAc, 0.1 N, pH = 6.8). The reaction was heated at 90 °C for 30 min to obtain ^{64}Cu-labeled peptide with 99% radiolabeling yield. The specific activity was 535.5 Ci/mmol.

Microfluidic radiolabeling was achieved on PDMS/glass radiolabeling chips. Ligand to metal ratio (2−7) was calculated based on the estimated specific activity of copper-64 production, which differed from batch to batch. Normally, the products from the first two runs of labeling reaction on microchip were discarded in order to establish the optimal labeling condition. After that, four to five repeated runs could be performed with consistent radiolabeling yields (>95%). The product was collected in an Eppendorf tube and examined by radio-HPLC. The delivered activity of the product was observed to drop with decreasing radiolabeling yields due to increased dose absorbed into the PDMS material. As expected, we observed about 45% retention of ^{64}Cu on the microchip after the experiment, which was consistent with our previous reports.[23]

Overall, the microfluidic radiolabeling has several advantages over conventional radiolabeling method: (a) microfluidic radiolabeling enables better handling of small reagent volumes (e.g., 4.5 μM/50 μL); (b) microfluidic radiolabeling requires a much lower ligand to metal ratio (2−7 vs 60), and only one-seventh of the ligand mass used in conventional labeling for each run (0.5 vs 3.7 μg), which greatly reduces the expensive cost of biomolecules such as peptides or antibodies; (c) it could achieve higher specific activity with above 95% labeling yields (ca. 850 vs 600 Ci/mmol); (d) it could perform reliable batchwise reactions with repeatable results (n = 4 or 5); (e) it provides efficient mixing by serpentine mixing channel which improves the reaction kinetics to shorten the reaction time (e.g., 10 min); (f) it provides fine control over reaction conditions due to automated control; (g) it requires a much smaller overall footprint of the system which minimizes the amount of space requiring shielding.

In Vitro Study. The cell binding study was performed using I^{125}-*Echistatin* binding assay. The results indicated that addition of the DOTA chelator, triazole moiety from "click" reaction, and triazine spacer into the molecule decreased the cyclo-(RGDfK) binding affinity to $\alpha_v\beta_3$ integrin receptors by increments of ca. 100 nM of IC_{50} value for each compound (Figures 2). The IC_{50} values were 421.9 ± 90.9, 509.7 ± 203.3, and 637.6 ± 113.5 nM for compounds DOTA-cyclo(RGDfK), DOTA-"Click"-cyclo(RGDfK) **15**, and DOTA-TZ-cyclo-(RGDfK) **14**, respectively, while plain cyclo(RGDfK) has IC_{50} value of 111.1 nM (data not shown).

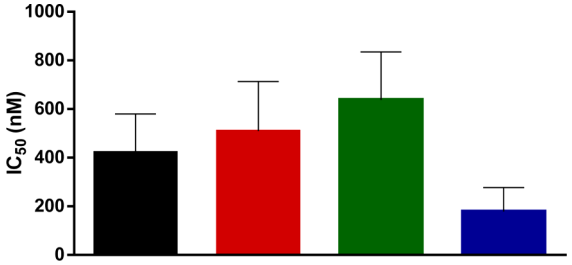

Figure 2. Competitive inhibition of IC_{50} toward I^{125}-*Echistatin* with DOTA-cyclo(RGDfK) (black, IC_{50} = 421.9 ± 90.9 nM), DOTA-"Click"-cyclo(RGDfK) **15** (red, IC_{50} = 509.7 ± 203.3 nM), DOTA-TZ-cyclo(RGDfK) **14** (green, IC_{50} = 637.6 ± 113.5 nM), and DOTA-TZ-Bis-cyclo(RGDfK) **13** (blue, IC_{50} = 178.5 ± 57.1 nM). (n = 3, standard error of mean.)

The DOTA-TZ-Bis-cyclo(RGDfK) **13** conjugated with two cyclo(RGDfK) peptides had the strongest binding affinity to the integrin $\alpha_v\beta_3$ receptors among this series of compounds with IC_{50} value of 178.5 ± 57.1 nM. The low IC_{50} value of DOTA-TZ-Bis-cyclo(RGDfK) **13** might be due to the bivalency effect of the compound,[3c] compared to DOTA-TZ-monocyclo(RGDfK). It had significantly increased integrin $\alpha_V\beta_3$ binding affinity, similar to the reported HYNIC-dimer (112 ± 21 nM),[18] and FPTA-RGD2 which contains two cyclo(RGDfK) peptide and one triazole moiety (144 ± 6.5 nM).[5]

Serum Stability Study. Both triazine-based compounds conjugated with one or two cyclo(RGDfK) peptides showed higher stability than DOTA-cyclo(RGDfK) or DOTA-"Click"-cyclo(RGDfK) **15** in rat serum. Compound DOTA-TZ-cyclo(RGDfK) **14** was observed to be stable in rat serum for the first 24 h, and then the stability decreased significantly to ca. 55% at 48 h (Figure 3). Compound DOTA-TZ-Bis-cyclo-

dx.doi.org/10.1021/bc500034n | Bioconjugate Chem. 2014, 25, 761−772

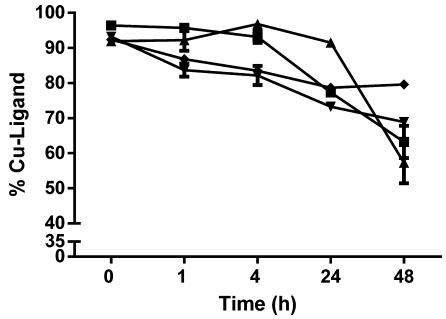

Figure 3. Serum stability study of peptide ^{64}Cu-DOTA-cyclo(RGDfK) (inverted pyramid), ^{64}Cu-DOTA-"Click"-cyclo(RGDfK) (diamond), ^{64}Cu-DOTA-TZ-cyclo(RGDfK) (triangle), and ^{64}Cu-DOTA-TZ-Bis-cyclo(RGDfK) (square).

(RGDfK) **13** was stable for the first 4 h (>90%), and then the percentage intact decreased to 60% over the next 44 h. Compounds DOTA-cyclo(RGDfK) and DOTA-"Click"-cyclo-(RGDfK) **15** demonstrated lower stability than the triazine-based conjugates in rat serum. The DOTA-"Click"-cyclo-(RGDfK) **15** conjugate had slightly lower stability than DOTA-TZ-Bis-cyclo(RGDfK) **13** for the first 4 h, and then it turned out to be unchanged for the next 44 h (76%). DOTA-cyclo(RGDfK) conjugate showed the lowest serum stability, but nevertheless very close to the behavior of DOTA-"Click"-cyclo(RGDfK) **15** in rat serum. Serum stability study showed that triazine-based compounds containing both triazole and triazine aromatic moieties were fairly stable in the rat serum environment for at least 4 h, then the stability dropped over time. These expected phenomena might be due to the transchelation challenge from copper-binding biomolecules present in the extracellular and intracellular environments.[19]

Biodistribution Study and Structure–Activity Evaluation. All four peptide conjugates had higher tumor uptake at 4 h than that at 1 h on homozygous Nu/Nu female athymic nude mice implanted with 5×10^6 U87MG cells. Compound DOTA-"Click"-cyclo(RGDfK) **15** had the highest tumor uptake among these four at 4 h p.i. with 1.90 ± 0.65%ID/g, followed by DOTA-cyclo(RGDfK) 1.65 ± 0.40%ID/g, DOTA-TZ-Bis-cyclo(RGDfK) **13** 1.15 ± 0.10%ID/g, and DOTA-TZ-cyclo-(RGDfK) **14** 0.86 ± 0.17%ID/g (Figure 4). The insertion of a

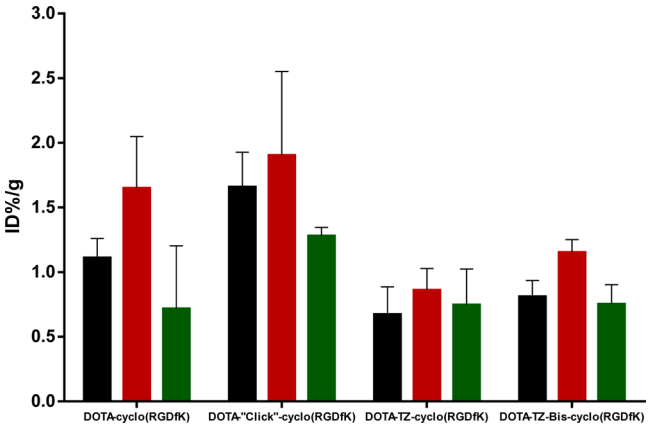

Figure 4. Tumor uptake of (A) ^{64}Cu-DOTA-cyclo(RGDfK); (B) ^{64}Cu-DOTA-"Click"-cyclo(RGDfK); (C) ^{64}Cu-DOTA-TZ-cyclo-(RGDfK); (D) ^{64}Cu-DOTA-TZ-Bis-cyclo(RGDfK) p.i.: 1 h (black); 4 h (red); 24 h (green).

triazole moiety made DOTA-"Click"-cyclo(RGDfK) **15** have higher specific targeting, also increased uptake in liver, kidney, and pancreas compared to DOTA-cyclo(RGDfK) (Figure 5).

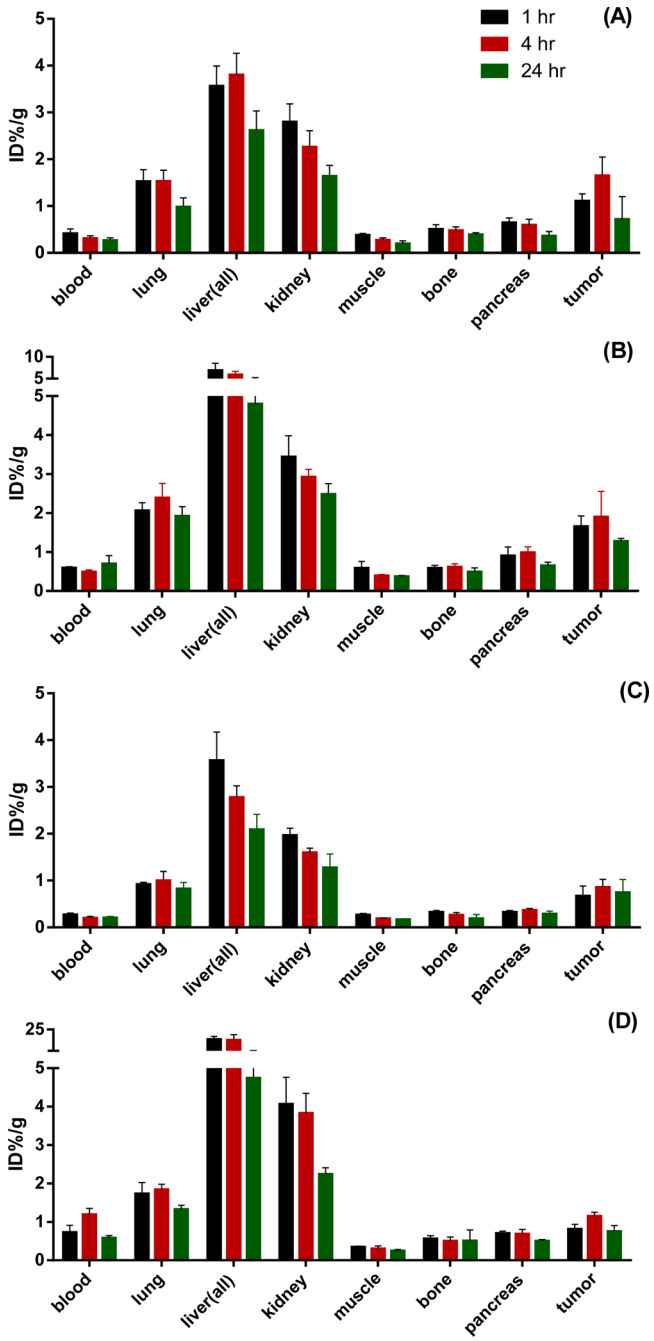

Figure 5. Biodistribution study of (A) ^{64}Cu-DOTA-cyclo(RGDfK); (B) ^{64}Cu-DOTA-"Click"-cyclo(RGDfK); (C) ^{64}Cu-DOTA-TZ-cyclo-(RGDfK); (D) ^{64}Cu-DOTA-TZ-Bis-cyclo(RGDfK).

We observed that DOTA-TZ-cyclo(RGDfK) **14** had lower liver, kidney, and pancreas uptake than DOTA-cyclo(RGDfK) at all time points studied. It can be inferred that the triazine moiety in DOTA-TZ-cyclo(RGDfK) **14** did not increase the nontumor organ uptake, although it had the lowest tumor uptake among these four. The liver washout of DOTA-TZ-cyclo(RGDfK) **14** was faster than DOTA-"Click"-cyclo-(RGDfK) **15**: the prior compound had decreasing liver uptake after 1 h p.i., while the latter one had highest liver uptake at 4 h

dx.doi.org/10.1021/bc500034n | Bioconjugate Chem. 2014, 25, 761–772

p.i. This was consistent with the measured log*D* values: DOTA-"Click"-cyclo(RGDfK) peptide (log*D* −3.3) had the highest lipophilicity among this series of peptide conjugates (Supporting Information Table S2), which increased the overall hepatic uptake and hepatobiliary excretion of the peptide conjugate or its radiocatabolites by specific biochemical pathway.[20] DOTA-TZ-Bis-cyclo(RGDfK) **13** (log*D* −4.1) displayed a similar trend of organ uptake over time to DOTA-TZ-cyclo(RGDfK) **14** (log*D* −3.6). However, contrary to our expectations, DOTA-TZ-Bis-cyclo(RGDfK) **13** had significantly increased liver uptake (e.g., 15.86 ± 2.71%ID/g at 1 h p.i.), and slightly increased kidney and pancreas uptake compared to DOTA-cyclo(RGDfK) (log*D* −4.3). A simple lipophilicity argument is obviously unable to explain this observation. The high liver uptake is similar to that observed with many RGD targeted nanoparticles and could be indicative of RES involvement perhaps through a specific bivalent binding to Kupffer cells; the monomeric RGD compounds are of much lower affinity and do not display this high uptake. Shuhendler et al. postulated that such an effect could explain the high liver uptake of RGD targeted nanoparticles.[21]

For the design of triazine-based cyclo(RGDfK) dimer conjugate, the two peptide motifs are separated by 22 bonds, which should be capable of binding two integrin $\alpha_v\beta_3$ receptors simultaneously.[3c] However, we were surprised to observe only a 20% increase of tumor uptake for dimer conjugate compared to the monomeric peptide conjugate based on triazine core at 1 h p.i. (0.81 ± 0.12 vs 0.67 ± 0.21) and 34% increase at 4 h p.i. (1.15 ± 0.10 vs 0.86 ± 0.17). We did not observe a clear bivalency effect for DOTA-TZ-BisRGD in the biodistribution study, although the *in vitro* study found a 3.6-fold enhancement of binding affinity on U87MG human glioblastoma cell. The observed bivalency effect shown *in vitro* was probably due to the high density of the integrin $\alpha_v\beta_3$ receptors on the glioblastoma tumor whole cell *in vitro*. A partial blocking effect was observed in the tumor with coinjection with unlabeled cyclo(RGDfK) (20 mg/kg body weight). The coinjected cold peptide blocked 41.7% tumor uptake of ^{64}Cu-DOTA-TZ-cyclo(RGDfK) which was radiolabeled by conventional method (0.35 ± 0.04%ID/g) and blocked 36.2% tumor uptake of ^{64}Cu-DOTA-TZ-Bis-cyclo(RGDfK) **13**, which was radiolabeled by microfluidic method (0.63 ± 0.16%ID/g).

Interestingly, DOTA-TZ-cyclo(RGDfK) **14** conjugate had the highest tumor to bone uptake ratio at all time points studied: 1.1 at 1 h p.i., 2.1 at 4 h p.i., and 3.5 at 24 h p.i. among all four compounds (Supporting Information Figure S3). Tumor to muscle uptake ratios for all four compounds were in the range of 2.3−3.0 at 1 h p.i. DOTA-cyclo(RGDfK) had the highest tumor/muscle uptake ratio as 6.1 at 4 h p.i. For the comparison of tumor to blood uptake ratio, DOTA-"click"-cyclo(RGDfK) **15** had highest value as 2.8 at 1 h p.i., while DOTA-cyclo(RGDfK) had the highest value as 5.3 at 4 h p.i. DOTA-TZ-Bis-cyclo(RGDfK) **13** had the lowest tumor/nontumor uptake ratio among these four compounds, probably due to unexpected low tumor uptake. DOTA-"click"-cyclo(RGDfK) **15** and DOTA-TZ-cyclo(RGDfK) **14** conjugates had rapid liver clearance for the first 4 h after the injection of ^{64}Cu labeled conjugates, while DOTA-cyclo(RGDfK) and DOTA-TZ-cyclo(RGDfK) **14** conjugates had slow liver clearance for the first 4 h (Supporting Information Figure S5). All the monomeric peptide conjugates had fast kidney clearance for the first 4 h, and then the uptake level became steady over next 20 h. Spacer linkers have been reported to play an important role in reducing nonspecific targeting and consequently increase the tumor/background ratio because of their hydrophilicity, acidity, or basicity;[18b,22] we did not observe significant advantages of short PEG linker (two CH_2CH_2O moieties) in our study. Longer hydrophilic PEG linkers might be a good choice in our case. Further studies are ongoing to understand the excretion pathway of the triazine-based conjugate and if any other factors play a role in the bivalency effect.

The ^{64}Cu labeled conjugate using the microfluidic method had moderately higher specific activity than that from using conventional radiolabeling method (850.9 ± 84.9 to 867.1 ± 88.0 Ci/mmol vs 535.5 to 612.5 Ci/mmol). The biodistribution results by injecting ^{64}Cu-labeled DOTA-TZ-Bis-cyclo(RGDfK) **13** conjugate demonstrated little differences in mice models using conventional or microfluidic radiolabeling method (Supporting Information Figure S4). It indicated that using microfluidic radiolabeling method could achieve at least the similar effect to conventional radiolabeling method while maintaining its intrinsic advantages.

■ CONCLUSIONS

We have developed a tool kit of triazine-based scaffold for diagnostic imaging purposes. We have demonstrated the synthesis of triazine-based monomeric and dimeric cyclo-(RGDfK) peptide conjugates containing the bifunctional chelator DOTA using "click chemistry". The methodology and techniques are versatile and provide a convenient method to switch different functionalities, e.g., PET imaging, optical imaging, targeting, or therapeutic group in the scaffold. In this report, we used cyclo(RGDfK) specifically targeting integrin $\alpha_v\beta_3$ as proof of principle. A dimeric cyclo(RGDfK) peptide was found to display significant bivalency effect in cellular study. The peptide was radiolabeled with ^{64}Cu using two different methods, microfluidic on-chip radiolabeling and conventional radiolabeling. The ^{64}Cu-DOTA-TZ-Bis-cyclo-(RGDfK) **13** using the microfluidic radiolabeling method had higher specific activity than the one using the conventional radiolabeling method. Biodistribution of all four conjugates in female athymic nude mice were evaluated. DOTA-"Click"-cyclo(RGDfK) **15** had the highest tumor uptake among these four at 4 h p.i. Further investigations need be done to re-evaluate the bivalency effect for the dimeric peptide conjugate *in vivo*.

■ EXPERIMENTAL SECTION

General. Peptide synthesis was performed on a Focus Xi peptide synthesizer (AAPPTec LLC, Louisville, KY). Microwave synthesis was performed on a Biotage Initiator Classic Microwave Synthesizer (Biotage LLC, Charlotte, NC). ^{1}H NMR and ^{13}C NMR spectrometry was performed on I400 Varian Inova (400 MHz for ^{1}H NMR and 100.5 MHz for ^{13}C NMR). MALDI-TOF mass spectrometry was performed on Voyager-DE STR BioSpectrometry Workstation (Applied Biosystems, San Francisco, CA). Accurate mass measurements were conducted on a Thermo Scientific (San Jose, CA) LTQ Orbitrap Velos mass spectrometer with Xcalibur operating system. The resolution of the instrument was set at 100,000 (m/z 400), and the instrument was externally calibrated before the electrospray ionization mass spectrometry (ESI-MS) analysis. Three microliter flow modular pump components (syringe pump, a pump driver circuit, and a power supply) were obtained from Harvard Apparatus (Holliston, MA). A Kapton-

insulated thin film heater (2 in. × 2 in.), Omega CN740 temperature controller, and an Omega SA 1-RTD probe were obtained from Omega Engineering (Stamford, CT). The BioScan AR-2000 radio-TLC plated reader was purchased from BioScan Inc. (Washington, DC). The ThermoMixer C was purchased from Eppendorf North America (Hauppauge, NY). Microliter syringes were obtained from Hamilton Co. (Reno, NV). A Capintec CRC-712 M radioisotope dose calibrator (Ramsey, NJ) and PerkinElmer 1480 Wizard 3″ Automatic Gamma Counter (Waltham, Massachusetts) were used for the measurement of radioactivity.

All solvents and reagents were purchased from commercial sources and used without further purification. The protected amino acids including Fmoc-Arg(Pbf)-OH, Fmoc-Lys(N_3)-OH, Fmoc-(D)-Phe-OH, and Fmoc-Asp(O^{t}Bu)-OH; cyclo-(RGDfK) peptide; and Fmoc-Gly-2Cl-Trt resin (200−400 mesh, 1% DVB, 0.77 meg/g) were purchased from AAPPTec LLC (Louisville, KY). DOTA-NHS-ester was purchased from Macrocyclics (Dallas, TX). All the other chemicals were purchased from Sigma-Aldrich (St. Louis, MO) or Fisher Scientific (Pittsburgh, PA). Deionized water (DI-H_2O) was produced in-house using a Millipore Milli-Q water system. $^{64}CuCl_2$ was produced at Washington University in St. Louis School of Medicine, and was obtained in a 0.1 M HCl solution. Silica TLC plates and C18 TLC silica plates were purchased from Sorbent Technologies (Norcross, GA). Analytical and semipreparative reverse phase high performance liquid chromatography (HPLC) was accomplished on a Hewlett-Packard 1050 series HPLC (Model 35900E) equipped with a single-channel high-sensitivity radiation detector (model 105s-1, Carroll & Ramsey Associates, Berkley, CA) and analyzed on Chem Station IC software (Agilent Technologies, Santa Clara, CA). The HPLC analytical column is an Econosil C18 reverse phase column (10 μm, 250 mm) from Alltech Associates, Inc. (Deerfield, IL). The HPLC semipreparative C4 reverse phase column (10 μm, 250 × 10 mm) was purchased from Higgins Analytical Inc. (Mountain View, CA). The flow rate was 1 mL/min for analytical HPLC and 2.5 mL/min for semipreparative HPLC, with the mobile phase of solvent A (0.1% TFA in water) and solvent B (0.1% TFA in acetonitrile). The UV detector was set at 220 nm. The gradient analytical HPLC method A (analytical) was starting from 10% B (0−2 min) to 90% B at 24 min (24−28 min), and returning to 10% B (30−32 min). Method B (analytical) was starting from 5% B (0−2 min) to 100% B (60 min), and finally to 5% (62 min). Method C (semipreparative) was starting from 5% B to 22% B (0−17 min), 25% B (47 min), 80% B (102−132 min), and finally to 5% (150 min).

Synthesis. *Spacer 1*. Cyanuric chloride (25 mg, 0.14 mmol) and *tert*-butyl-(2-(2-(2-aminoethoxy)ethoxy)ethyl)carbamate (33.50 mg, 0.15 mmol) were dissolved in anhydrous THF (1 mL) at 0 °C. *N,N*-Diisopropylethylamine (DIPEA, 52 μL, 0.30 mmol) was added to the reaction solution slowly at 0 °C under inert atmosphere. The reaction solution was stirred for 1.5 h at 0 °C. White solid was removed by filtration, and the solvent was removed under vacuum. The crude product was purified by silica chromatography (methanol/dichloromethane 5:95) and obtained as a yellowish viscous liquid (83 mg, 78%). ^{1}H NMR (400 MHz, $CDCl_3$): δ 6.80 (br, 1H), 3.66−3.54 (m, 10H), 3.34 (s, 2H), 1.43 (s, 9H). ^{13}C NMR (100.5 MHz, $CDCl_3$): δ 169.78, 165.61, 155.96, 79.12, 70.32, 41.22, 40.23, 28.30. HRMS (ESI): calcd for $C_{14}H_{24}Cl_2N_5O_4$ $[M+H]^+$: 396.1200; found: 396.1199.

Spacer 2. Spacer **1** (30 mg, 0.08 mmol), 2-(2-(prop-2-yn-1-yloxy)ethoxy)ethan-1-amine (65 mg, 0.23 mmol), and DIPEA (79 μL, 0.23 mmol) were dissolved in acetonitrile (2.5 mL), and charged into a thick-walled vessel. The reaction was heated at 140 °C for 90 min until the reaction was completed under microwave irradiation. The reaction solution was cooled to room temperature, and concentrated under vacuum. The product was further purified with silica chromatography (methanol/dichloromethane 5:95) to afford a viscous liquid (38 mg, 82%). ^{1}H NMR (400 MHz, $CDCl_3$): δ 4.18 (s, 4H), 3.66−3.53 (m, 26H), 3.29 (s, 2H), 2.43 (s, 2H), 1.42 (2, 9H). ^{13}C NMR (100.5 MHz, $CDCl_3$): 165.75, 161.11, 156.06, 79.56, 74.58, 70.11, 69.01, 58.35, 40.26, 28.39. MALDI-TOF: calcd for $C_{28}H_{47}N_7O_8$ $[M]^+$: 609.35; found: 609.51. HRMS (ESI): calcd for $C_{28}H_{48}N_7O_8$ $[M+H]^+$: 610.3559; found: 610.3560.

Spacer 3. Cyanuric chloride (100 mg, 0.55 mmol) was dissolved in anhydrous acetonitrile (2 mL), and the vessel was charged with nitrogen and cooled in ice bath. 2-(2-(Prop-2-yn-1-yloxy)ethoxy) ethan-1-amine (204 mg, 1.43 mmol) and DIPEA (247.6 μL, 1.43 mmol) were added, and then the ice bath was removed. The reaction solution was stirred at room temperature for another 5 h. The solution was concentrated and the crude product was purified with flash column chromatography (methanol/dichloromethane 1:99) to afford a white waxy solid (0.20 g, 90%). ^{1}H NMR (400 MHz, $CDCl_3$): δ 4.09 (d, J = 2.0 Hz, 4H), 3.58−3.51 (m, 16H), 2.39 (t, J = 2.2 Hz, 2H). ^{13}C NMR (100.5 MHz, $CDCl_3$): 169.8, 165.7, 79.60, 74.86, 70.29, 69.46, 69.07, 58.44, 40.62. MALDI-TOF: calcd for $C_{17}H_{24}ClN_5O_4$ $[M]^+$: 397.15; found: 397.39. HRMS (ESI): calcd for $C_{17}H_{25}ClN_5O_4$ $[M+H]^+$: 398.1590; found 398.1585.

Spacer 4. Spacer **1** (40 mg, 0.10 mmol) was dissolved in acetonitrile (2.5 mL) under inert atmosphere. A solution of linker 3 (18.4 mg, 0.12 mmol) in acetonitrile (1 mL) and DIPEA (28.7 μL, 0.15 mmol) was added to the reaction solution in two portions with a 30 min interval. The reaction was heated to 55 °C for 3 h and allowed to react until the reaction was completed. The solvent was removed under vacuum and the residue was purified with silica chromatography (methanol/dichloromethane 5:95) to afford the product as a white waxy solid (48 mg, 93%). ^{1}H NMR (400 MHz, $CDCl_3$): δ 4.20 (s, 2H), 3.67−3.54 (m, 18H), 3.33 (s, 2H), 2.45 (s, 1H), 1.43 (s, 9H). ^{13}C NMR (100.5 MHz, $CDCl_3$): δ 169.17, 168.43, 165.56, 156.04, 79.43, 74.69, 70.38, 70.23, 69.40, 68.99, 58.44, 40.60, 40.32, 28.36. HRMS (ESI): calcd for $C_{21}H_{36}ClN_6O_6$ $[M+H]^+$: 503.2379; found: 503.2382.

Spacer 5. Spacer **4** (20 mg, 0.04 mmol), 2-ethoxyethylamine (21 μL, 0.20 mmol), and DIPEA (35 μL, 0.20 mmol) were dissolved in acetonitrile (4 mL), and charged into a thick-walled vessel. The reaction was heated at 140 °C for 90 min under microwave irradiation until the reaction was completed. The reaction solution was cooled to room temperature, and concentrated under vacuum. The product was further purified with silica chromatography (methanol/dichloromethane 5:95) to afford a viscous liquid (21.6 mg, 95%). ^{1}H NMR (400 MHz, $CDCl_3$): δ 4.17 (s, 2H), 3.66−3.45 (m, 24H), 2.85 (s, 2H), 2.43 (s, 1H), 1.41 (s, 9H), 1.16 (t, J = 6.8 Hz, 3H). ^{13}C NMR (100.5 MHz, $CDCl_3$): 165.90, 156.05, 79.54, 79.05, 74.56, 70.19, 70.08, 69.32, 68.98, 66.31, 58.33, 53.36, 40.36, 40.23, 28.36, 15.07. MALDI-TOF: calcd for $C_{25}H_{45}N_7O_7$ $[M]^+$: 555.34; found: 554.97. HRMS (ESI): calcd for $C_{25}H_{46}N_7O_7$ $[M+H]^+$: 556.3453; found 556.3454.

Spacer 6. Cyanuric chloride (157.7 mg, 0.86 mmol) and 2-(2-(prop-2-ynyloxy)ethoxy)ethan-1-amine (123.3 mg, 0.86

dx.doi.org/10.1021/bc500034n | *Bioconjugate Chem.* 2014, 25, 761−772

mmol) were dissolved in dry THF at 0 °C under nitrogen flow. Then DIPEA (200 μL, 1.10 mmol) was added to the reaction solution slowly. The reaction solution was stirred for 1 h and monitored by TLC. The solvent was removed under vacuum and the residue was purified with silica chromatography (methanol/dichloromethane 2:98) to afford a white waxy solid (0.19 g, 76%). ^{1}H NMR (400 MHz, $CDCl_3$): δ 6.16 (br, 1H), 4.19 (d, J = 2.4 Hz, 2H), 3.66 (d, J = 4.8 Hz, 8H), 2.45 (s, 1H). ^{13}C NMR (100.5 MHz, $CDCl_3$): 170.18, 166.04, 79.63,75.19, 70.61, 69.31, 69.23, 58.74, 41.53. HRMS (ESI): calcd for $C_{10}H_{12}C_{l2}N_4O_2$ $[M+H]^+$: 291.0410; found: 291.0410.

Spacer 7. A mixture of spacer **6** (0.13 g, 0.45 mmol), 2-ethoxyethylamine (0.06 g, 0.65 mmol), and DIPEA (0.06 g, 0.45 mmol) were mixed in anhydrous acetonitrile (1 mL). The reaction solution was stirred at room temperature. After 2 h, the reaction was complete as determined by TLC. The reaction solution was concentrated and the residue was purified by chromatography with silica gel eluted by 2% dichloromethane/methanol. The product was obtained as a viscous liquid (0.14 g, 93%). ^{1}H NMR (400 MHz, $CDCl_3$): δ 4.11 (d, J = 2.0, 2H), 3.61−3.42 (m, 14H), 2.40 (t, J = 2.4 Hz, 1H), 1.10 (t, J = 7.0 Hz, 3H). ^{13}C NMR (100.5 MHz, $CDCl_3$): 167.81, 165.39, 165.35, 70.02, 69.19, 68.78, 68.31, 66.25, 58.16, 40.39, 14.87. MALDI-TOF: calcd for $C_{14}H_{22}ClN_5O_3$ $[M]^+$: 343.14; found: 343.69. HRMS (ESI): calcd for $C_{14}H_{23}ClN_5O_3$ $[M]^+$: 344.1484; found: 344.1478.

Spacer 8. Method 1. Spacer **3** (33 mg, 49.2 mmol) was dissolved in dichloromethane/TFA (1/1, 2 mL) and the solution was stirred for 1 d at room temperature. The solvent was removed under vacuum and the residue was redissolved in sat. sodium bicarbonate. The product was extracted by dichloromethane (10 mL × 3), and the organic phase was washed by water (1 mL × 3) until its pH is neutral. The organic layer was dried over anhydrous sodium sulfate. The solution was filtered and concentrated. The residue was dissolved in acetone and filtered over a Celite cake. The product was further purified by HPLC (Method A) to afford a viscous liquid (22 mg, 88%).

Method 2. Spacer **3** (0.18 g, 0.45 mmol), 2,2′-(ethylenedioxy)bis(ethylamine) (2.64 mL, 18.12 mmol), and DIPEA (1.58 mL, 9.06 mmol) were mixed in anhydrous acetonitrile (50 mL) under nitrogen flow. The reaction mixture was heated at 80 °C for 3 h until the reaction was complete as determined by TLC. The reaction solution was concentrated to dryness and redissolved in dichloromethane (100 mL). The organic layer was washed with DI-H_2O (20 mL × 1), sodium bicarbonate (20 mL × 2), and DI-H_2O (20 mL × 2). The organic layer was dried over anhydrous sodium sulfate. The solvent was removed under vacuum and the residue was purified with flash column chromatography (silica, methanol/dichloromethane 5:95 then triethylamine/methanol/dichloromethane 2:10:88). The product was obtained as a viscous liquid (0.21 g, 89%). ^{1}H NMR (400 MHz, $CDCl_3$): δ 5.19 (br, 3H), 4.17 (s, 2H), 4.12 (d, J = 2.4 Hz, 4H), 3.61−3.47 (m, 26H), 2.93 (s, 2H), 2.41 (t, J = 2.4 Hz, 2H). ^{13}C NMR (100.5 MHz, $CDCl_3$): 165.69, 79.42, 74.56, 69.96, 69.94, 69.86, 69.66, 68.83, 58.17, 45.80, 40.42, 40.05. MALDI-TOF: calcd for $C_{23}H_{39}N_7O_6$ $[M]^+$: 509.30; found: 509.23. HRMS (ESI): calcd for $C_{23}H_{40}N_7O_6$ $[M+H]^+$: 510.3035; found: 510.3036.

Spacer 9. Method 1. Spacer **5** (33 mg, 59.40 mmol) was dissolved in dichloromethane/TFA (1:1, 2 mL) and the solution was stirred for 1 d at room temperature. The solvent was removed under vacuum and the residue was redissolved in sat. sodium bicarbonate. Dichloromethane was used to extract the product, and water (1 mL × 3) to wash the organic phase until the pH 7. The organic layer was dried over anhydrous sodium sulfate. The solution was filtered and concentrated. The residue was dissolved in acetone and filtered over a Celite cake. The product was further purified by HPLC (Method A) to afford a viscous liquid (24 mg, 90%).

Method 2. Spacer **7** (0.14 g, 0.41 mmol), 2,2′-(ethylenedioxy)bis(ethylamine) (2.36 mL, 16.10 mmol), and DIPEA (1.42 mL, 8.20 mmol) were mixed in anhydrous acetonitrile (10 mL) under nitrogen flow. The reaction mixture was heated at 80 °C for 3 h until the reaction was found complete by TLC. The reaction solution was concentrated to dryness and redissolved in dichloromethane (50 mL). The organic layer was washed with DI-H_2O (10 mL × 1), sodium bicarbonate (10 mL × 2), and DI-H_2O (10 mL × 2). The organic layer was dried over anhydrous sodium sulfate. The solvent was removed under vacuum and the residue was purified with flash column chromatography (silica, methanol/dichloromethane 5:95, then triethylamine/methanol/dichloromethane 2:10:88). The product was obtained as a viscous liquid (0.16 g, 86%). ^{1}H NMR (400 MHz, $CDCl_3$): δ 5.84−5.18 (br, 3H), 4.17 (s, 2H), 3.67−3.44 (m, 24H), 2.84 (t, J = 5.0 Hz, 2H), 2.43 (t, J = 2.4 Hz, 1H), 1.97 (br, 2H), 1.16 (t, J = 6.8 Hz, 3H). ^{13}C NMR (100.5 MHz, $CDCl_3$): 166.30, 79.87, 74.93, 73.68, 70.57, 70.55, 70.49, 70.46, 70.41, 69.70, 69.31, 66.66, 58.67, 41.98, 40.66, 40.55. MALDI-TOF: calcd for $C_{20}H_{37}N_7O_5$ $[M]^+$: 455.29; found: 455.22. HRMS (ESI): calcd for $C_{20}H_{38}N_7O_5$ $[M+H]^+$: 455.2929; found: 455.2926.

Cyclo(RGDfK)-N_3. The Fmoc-Gly-2Cl-Trt resin (0.40 g, 0.31 mmol) was loaded on Focus Xi peptide synthesizer. Protected amino acid Fmoc-Arg(Pbf)-OH (0.60 g, 0.93 mmol), Fmoc-Lys(N_3)-OH (0.37 g, 0.93 mmol), Fmoc-(D)Phe-OH (0.36 g, 0.93 mmol), and Fmoc-Asp(O^{t}Bu)-OH (0.38 g, 0.93 mmol) was coupled onto the resin subsequently with 3 mol equiv relative to the resin by using HBTU/DMF (0.4 M) and DIPEA/DMF (2 M). Piperidine/DMF (20%) was used to deprotect the Fmoc group from C-terminal after each coupling reaction. The Kaiser test was performed after each coupling reaction. After automated synthesis, the peptide was cleaved from the resin using a prepared cocktail (30 mL, acetic acid: 2,2,2-trifluoroethanol:dichloromethane 6:6:18). The resin was suspended in the cocktail solution and the solution was shaken for 1 h. The resin was then filtered on a fine frit funnel. The liquid was concentrated under vacuum and the acetic acid was removed by azeotroping with toluene (∼200 mL). The concentrated peptide residue was added dropwise to cold ethyl ether solution (∼100 mL). A light yellow solid formed and was filtered through a frit funnel. The solid was washed with cold ether 3 times, and dried in vacuo for 2 h to afford a crude linear peptide (0.23 g). A 500 mL 2-neck round-bottom flask was filled with dichloromethane (150 μL), 4-dimethylaminopyridine (18.2 mg, 0.15 mmol), propylphosphonic anhydride (≥50 wt %, in ethyl acetate, 1.3 mL, 2.18 mmol), and triethylamine (1.5 mL, 10.70 mmol). The linear peptide was dissolved in dichloromethane (8 mL) and the solution was added dropwise through an addition funnel for 4 h. The reaction solution was stirred overnight. The solvent was removed under vacuum and the residue was dried under vacuum for 3 h. The crude cyclized peptide was put into a round-bottom flask, and a solution of deprotection cocktail of trifluoroacetic acid (14 mL, 0.18 mmol, 95%), water (1 mL), and DL-dithiothreitol (0.32 g, 2.0 mmol) was added to the flask.

The reaction solution was stirred for 30 min at room temperature. Then the solution was diluted with ice-cold diethyl ether solution. A white solid was precipitated and filtered with a fine fritted funnel. The solid was washed with cold ether and dried overnight. The crude solid was further purified with semipreparative HPLC (reverse phase C18, Method C), the fractions were collected and lyophilized to afford a white fluffy solid (60.10 mg, overall yield 31%). HRMS (ESI): calcd for $C_{27}H_{39}N_{11}O_7$ $[M+H]^+$: 630.3104; found: 629.3034.

NH_2-TZ-Bis-cyclo(RGDfK) ***10***. Copper sulfate (10 mM, 42 uL) was added to a sodium ascorbate solution (50 mM, 42 μL). The copper(I) solution was vortexed and allowed to sit for 5 min. The TBTA acetonitrile solution (18.9 mM, 56 μL) was added to the copper(I) solution to make a TBTA-Cu (I) complex solution. Spacer **8** (1.5 mg, 2.90 μmol) was added to the Cu (I)-ligand solution. After 2 min, cyclo(RGDfK)-N_3 peptide (5.0 mg, 7.90 μmol) was added to a methanol/water solution (1/1, 0.8 mL). The whole reaction was heated at 100 °C with microwave irradiation for 1 h. The reaction solution was concentrated and the residue was purified by HPLC (Method B, t_R = 21.47 min), and lyophilized to afford the product (4.5 mg, 90%). MALDI-TOF: calcd for $C_{77}H_{117}N_{29}O_{20}$ $[M]^+$: 1767.90; found: 1766.04. HRMS (ESI): calcd for $C_{77}H_{118}N_{29}O_{20}$ $[M+H]^+$: 1768.9102, found: 1768.9077; $[M+H]^{2+}$: 884.9588; found: 884.9587.

NH_2-TZ-cyclo(RGDfK) ***11***. Copper sulfate (10 mM, 28 uL for 0.28 μmol) was added to a sodium ascorbate solution (50 mM, 28 μL for 1.40 umol). The copper(I) solution was vortexed and allowed to sit for 5 min. The TBTA acetonitrile solution (18.9 mM, 37 μL for 0.70 μmol) was added to the Cu (I) solution to make a TBTA-Cu (I) complex solution. Spacer **9** (0.95 mg, 2.10 μmol) was added to the Cu (I)-ligand solution. After 2 min cyclo(RGDfK)-N_3 peptide (1.8 mg, 2.80 μmol) was added to the reaction solution of methanol/water (1:1, 0.5 mL). The whole reaction was heated at 100 °C with microwave irradiation for 40 min. The reaction solution was concentrated and the residue was purified by HPLC (Method A, t_R = 11.48 min), and lyophilized to afford the product (1.8 mg, 79%). MALDI-TOF: calcd for $C_{47}H_{76}N_{18}O_{12}$ $[M]^+$: 1084.59, found: 1084.16. HRMS (ESI): calcd for $C_{47}H_{76}N_{18}O_{12}K$ $[M+K]^+$: 1123.5522; found: 1123.4601.

NH_2-"Click"-cyclo(RGDfK) ***12***. Copper sulfate (10 mM, 110 uL for 1.1 μmol) was added to a sodium ascorbate solution (50 mM, 110 μL for 5.50 umol). The Cu (I) solution was vortexed and sit for 5 min. The TBTA acetonitrile solution (18.9 mM, 145 μL for 2.75 μmol) was added to the copper(I) solution to make the TBTA-Cu (I) complex solution. Propargyl amine (0.6 mg, 0.01 mmol) was added to the Cu (I)-ligand solution. After 2 min cyclo(RGDfK)-N_3 peptide (7.6 mg, 0.01 mmol) was added to the reaction solution of methanol/water (1:1, 3 mL). The whole reaction was heated under 100 °C microwave condition for 20 min. The reaction solution was concentrated. The residue was purified by HPLC (Method A, t_R = 9.71 min), and lyophilized to afford the product (4.3 mg, 54%). MALDI-TOF: calcd for $C_{30}H_{44}N_{12}O_7$ $[M+H]^+$: 685.35; found: 685.13; $[M+H_2O]^+$: 702.36, found: 702.03. HRMS (ESI): calcd for $C_{30}H_{44}N_{12}O_7$ $[M+H]^+$: 685.3529; found: 685.3525.

DOTA-TZ-Bis-cyclo(RGDfK) ***13***. DOTA-NHS ester (4.7 mg, 6.20 μmol) was added to a 1 mL vessel. The vessel was charged with nitrogen and NH_2-TZ-Bis-cyclo(RGDfK) **10** (4.3 mg, 2.4 μmol) dissolved in anhydrous DMF (250 μL) was added to the solution. DIPEA (6.6 μL, 37.80 μmol) was added to the solution, and the reaction was monitored by MALDI mass spectrometer. After 24 h, DI-H_2O (200 μL) was added to the reaction solution, and the solution was stirred for 30 min. After that, the whole solution was filtered through a syringe filter (0.24 μm). The product was purified by HPLC (Method B, t_R = 19.52 min), and dried by lyophilization to afford a white fluffy solid (2.5 mg, 48%). HRMS (ESI): calcd for $C_{93}H_{143}N_{33}O_{27}$ $[M+H+K]^{2+}$: 1097.0268; found: 1097.0223.

DOTA-TZ-cyclo(RGDfK) ***14***. DOTA-NHS ester (5.2 mg, 6.80 μmol) was added to a 1 mL vessel. The vessel was charged with nitrogen and NH_2-TZ-cyclo(RGDfK) **11** (3 mg, 2.70 μmol) was dissolved in anhydrous DMF (200 μL). DIPEA (7.6 μL, 43.50 μmol) was added to the solution, and the reaction was monitored by MALDI mass spectrometer. After 24 h, DI-H_2O (150 μL) was added to the reaction solution, and the solution was stirred for 30 min. After that, the whole solution was filtered through a syringe filter (0.24 μm). The product was purified by HPLC (Method B, t_R = 18.76 min), and dried by lyophilization to afford a white fluffy solid (1.8 mg, 45%). MALDI-TOF: calcd for $C_{63}H_{102}N_{22}O_{19}$ $[M+H]^+$: 1471.78; found: 1471.71. HRMS (ESI): calcd for $C_{63}H_{102}N_{22}O_{19}$ $[M-2H+K]^-$: 1507.7178; found: 1507.7144.

DOTA-"Click"-cyclo(RGDfK) ***15***. DOTA-NHS ester (3.6 mg, 4.70 μmol) was added to a 1 mL vessel. The vessel was charged with nitrogen and NH_2-"Click"-cyclo(RGDfK) **12** (2.7 mg, 3.90 μmol) dissolved in anhydrous DMF (200 μL) was added to the solution. DIPEA (6.6 μL, 37.80 μmol) was added to the solution, and the reaction solution was stirred at room temp overnight. After the reaction, DI-H_2O (100 μL) was added to the reaction solution, and the solution was stirred for 30 min. After that, the whole solution was filtered through a syringe filter (pore size 0.24 μm). The product was purified by HPLC (Method B, t_R = 15.51 min) and dried by lyophilization to afford a white fluffy solid (2.7 mg, 64%). MALDI-TOF: calcd for $C_{46}H_{70}N_{16}O_{14}$ $[M]^+$: 1070.53, found: 1070.63; $[M+H_2O]^+$: 1088.54, found: 1088.56. HRMS (ESI): calcd for $C_{46}H_{70}N_{16}O_{14}$ $[M-2H+K]^-$: 1107.4743; found: 1107.4651.

PDMS/Glass Chip Fabrication. The radiolabeling chip is a PDMS-based microreactor. The design of the chip contains three major components: (1) a staggered herringbone mixing channel which passively mixes reagents; (2) five incubation reservoirs for the radiometal−ligand mixture; (3) a thin-film heater for heating the reaction mixture. The fabrication of the chip was described in detail in our previous publication.[23]

Conventional and Microfluidic $^{64}Cu^{2+}$ Radiolabeling. *Conventional Radiolabeling.* $^{64}CuCl_2$ in 0.1 M HCl was added to a sodium acetate buffer (0.1 M, pH 6.8). DOTA conjugated cyclo(RGDfK) peptides (0.0017 μmol) were mixed with $^{64}Cu(OAc)_2$ stock solution (1 mCi) in sodium acetate buffer solution (~200 μL in total volume). The reaction solution was incubated on a ThermoMixer (700 rpm) at 90 °C for 30 min. No further purification was performed. The radiolabeling yield was determined by radio-TLC and radio-HPLC (>95%). The specific activity of radiolabeled compounds was ca. 550 Ci/mmol.

Microfluidic Radiolabeling. The radiometal, ligand, and buffer solution were pumped into the microreactor through three separate inlets. The solutions were mixed in the staggered herringbone mixing channels by chaotic advection induced by the geometry of the herringbones.[24] The mixed reagents then filled a series of hexagonal reservoirs and the reaction mixture was incubated at a desired temperature for a specified time. The reaction product was flushed out by injecting a sodium acetate

buffer solution (0.1 M, pH 6.8) into the microreactor. The syringe pumps were controlled by a LabVIEW virtual instrument (VI). The flow rates, incubation time, desired volume of the product (52.6 μL for the total volume of the holding tanks), and the stoichiometric molar ratios of buffer, radiometal, and ligand were controlled through the VI. A thin-film heater was placed underneath the glass surface of the microreactor. A temperature controller and a resistance temperature detector (RTD) probe were used to maintain the temperature within ±1 °C of the desired temperature. The radiometal syringe pump, heater, and microreactor were shielded with lead shielding (2″ thick). The syringes were connected to the reactor with Hamilton Luer Lock 30 gauge PTFE tubing of one foot length.

The PDMS/glass radiolabeling chip was first washed with diluted nitric acid solution (1 N, 1 mL × 3) at a flow rate 30 μL/min, to remove any metal ions bound nonspecifically to the chip surfaces. Then the chip was washed with water and sodium acetate buffer (0.1 N, pH 6.8) separately (1 mL × 3). All Hamilton glass syringes (250 and 500 μL) and disposable plastic syringes (1 mL × 3) were rinsed with nitric acid (1 N, 1 mL × 3), water, and sodium acetate buffer (0.1 N, pH 6.8, 1 mL × 3) subsequently. $^{64}Cu(OAc)_2$ solution (5 mCi, 250 μL), DOTA-TZ-Bis-cyclo(RGDfK) **13** peptide stock solution (13.5 μM, 250 μL), and sodium acetate buffer (0.1 M, 1 mL) were loaded into syringes and installed on the syringe pumps. The radiometal, ligand, and buffer solutions were controlled to mix in the chip with different volume ratio using LabVIEW interface software. The total volume was set to 52.6 μL and the total flow rate was set to 25 μL/min. After each reaction, three chip volumes of buffer solution were pumped into the chip to wash the holding tanks thoroughly. The reaction temperature was set to 37 °C and the residence time was set to 10 min. After collecting the product, the activity was measured by dose calibrator (~200 μCi, Capintec Inc. NJ), and the yield of radiolabeling reaction was determined by radio-TLC and radio-HPLC. The first two on-chip reactions were discarded in order to stabilize the chip condition. Radiolabeling was repeated for 4–5 times under the same condition. The radiolabeling yield was determined by radio-TLC and radio-HPLC (>97%). The specific activity of radiolabeled compounds was calculated ca. 850 Ci/mmol.

Cell Culture and *in Vitro* Binding Assay. The *in vitro* cell binding assay was performed with U87MG human glioblastoma cell line. U87MG human glioblastoma cells were grown in Dulbecco's medium (Gibco) supplemented with 10% fetal bovine serum (FBS). The affinities of cyclo(RGDfK) conjugates for $\alpha_v\beta_3$ integrin were examined via competitive cell binding assay using ^{125}I-*echistatin* as the integrin $\alpha_v\beta_3$-specific radioligand. To determine the *in vitro* binding affinity of cyclo(RGDfK) peptide conjugates, U87MG cells were harvested for membrane preparations as previously described.[25] Protein concentrations were determined using the Pierce Non-Reducing Agent Compatible Kit (Rockford, IL). Briefly, 25 μg of membrane protein in 100 μL binding buffer (10 mM HEPES, 5 mM $MgCl_2$, 1 mM EDTA, 0.1% BSA, 10 μg/mL leupeptin, 10 μg/mL pepstatin, 0.5 μg/mL aprotinin, and 200 μg/mL bacitracin, pH 7.4) was applied to 0.1% polyethyleneimine-pretreated wells of a 96-well Multiscreen Durapore filtration plate (Millipore Corp., Bedford, MA) via vacuum manifold aspiration. The wells were then washed three times with washing buffer (10 mM HEPES, 1 mM EDTA, 5 mM $MgCl_2$, 0.1% BSA). Increasing concentrations of cyclo(RGDfK) peptide (0–91 μM) were added in a volume of 10 μL to triplicate wells. To each well, 0.279 kBq of ^{125}I-*Echistatin* (PerkinElmer, Boston, MA) in a volume of 100 μL was added. The plate was incubated at room temperature for 1 h, after which the wells were washed twice with washing buffer. The membranes were dried, removed, and placed in separate tubes for determination of bound radioactivity. The membrane-associated radioactivity was determined using a Packard II γ counter (PerkinElmer, Waltham, MA). The IC_{50} values were calculated by fitting the data using nonlinear regression in GraphPad Prism Software (San Diego, CA).

Octanol/Water Partition Coefficient. The octanol and buffer solution (0.01 M ammonium acetate, pH 6.8) were mixed and saturated for 1 d. The partition coefficients were determined by adding 8 μL of ^{64}Cu-labeled peptide conjugate (20 μCi) to a solution containing 500 μL sat. octanol and 492 μL sat. buffer. The mixed solutions were vortexed for 5 min, and then centrifuged for 5 min at 3000 rpm. Aliquots (100 μL) of octanol and buffer were removed, weighed, and counted by gamma counter. The partition coefficient was calculated as a ratio of counts in the octanol fraction of unit mass to counts in the buffer fraction of unit mass. The experiments were performed in triplicate, and the average Log*D* value was reported.

Serum Stability Study. The *in vitro* serum stabilities of the ^{64}Cu-cyclo(RGDfK) conjugated compounds were evaluated by incubation with freshly isolated lean rat serum. Each ^{64}Cu-radiolabeled cyclo(RGDfK) conjugated compound (9 μM, 100 μCi) was mixed with rat serum (100 μL) in a 1.5 mL centrifuge tube. The reaction was incubated on an Eppendorf ThermoMixer C (Hauppauge, NY) at 37 °C (300 rpm). Aliquots were withdrawn at 0, 1, 4, 24, and 48 h, and evaluated by radio-TLC on a BioScan AR-2000 Imaging Scanner (Washington, DC). The radio-TLC was analyzed on reverse phase C18 silica plates using 1:1 methanol/5% ammonium formate. The reactions were repeated in triplicate.

Animal Model and Biodistribution Studies. Animal studies were performed in accordance with the guidelines for the care and use of research animals as defined by the Washington University Animal Studies Committee. Homozygous Nu/Nu female athymic nude mice at 6–7 weeks of age were implanted subcutaneously on the rear flank with 5×10^6 U87MG cells in a volume of 100 μL saline. Tumors were allowed to grow for 14 d, upon which the mice (n = 3) were injected intravenously with 10 μCi of respective ^{64}Cu-labeled cyclo(RGDfK) peptide conjugates. One group was coinjected with 350 μg of cold cyclo(RGDfK) peptide to do the blocking study. Mice were sacrificed at 1 and 4 h post injection. Blood, lung, liver, kidney, muscle, bone, pancreas, and tumor were collected for determination of tissue-associated radioactivity. Counts were obtained using a γ-counter. The percent injected dose per gram (%ID/g) for each tissue was calculated to normalization from a standard dose.

■ ASSOCIATED CONTENT

Supporting Information

Synthesis, TBTA, and DOTA competitive binding study, reactions of "clickable" DOTA-triazine spacer, determination of partition coefficient, and in vivo study. This material is available free of charge via the Internet at http://pubs.acs.org.

AUTHOR INFORMATION

Corresponding Author

*Phone: 314-362-8461, Fax: 314-362-9940, E-mail: ReichertD@wustl.edu.

Notes

The authors declare no competing financial interest.

ACKNOWLEDGMENTS

We acknowledge financial support from National Institutes of Health (5R01CA161348). We also thank Dr. Fong-Fu Hsu at WUSTL-School of Medicine Biomedical Mass Spectrometry Facility for the assistance of high resolution electrospray ionization mass spectrometry. Part of this work made use of the facilities in the Frederick Seitz Materials Research Laboratory Central Facilities and Micro-Nano-Mechanical Systems Cleanroom at University of Illinois at Urbana−Champaign, which is partially supported by the U.S. Department of Energy under grants DE-FG02-07ER46453 and DE-FG02-07ER46471.

REFERENCES

(1) (a) Gasparini, G., Brooks, P. C., Biganzoli, E., Vermeulen, P. B., Bonoldi, E., Dirix, L. Y., Ranieri, G., Miceli, R., and Cheresh, D. A. (1998) Vascular integrin alpha(v)beta(3): A new prognostic indicator in breast cancer. *Clin. Cancer Res. 4* (11), 2625−2634. (b) Ellis, L. M., and Fidler, I. J. (1996) Angiogenesis and metastasis. *Eur. J. Cancer 32A* (14), 2451−2460. (c) Brooks, P. C. (1996) Role of integrins in angiogenesis. *Eur. J. Cancer 32A* (14), 2423−2429.

(2) (a) Haukkala, J., Laitinen, I., Luoto, P., Iveson, P., Wilson, I., Karlsen, H., Cuthbertson, A., Laine, J., Leppanen, P., Yla-Herttula, S., Knuuti, J., and Roivainen, A. (2009) Ga-68-DOTA-RGD peptide: biodistribution and binding into atherosclerotic plaques in mice. *Eur. J. Nucl. Med. Mol. Imaging 36* (12), 2058−2067. (b) Decristoforo, C., Gonzalez, I. H., Carlsen, J., Rupprich, M., Huisman, M., Virgolini, I., Wester, H. J., and Haubner, R. (2008) (68)Ga- and (111)In-labelled DOTA-RGD peptides for imaging of alpha v beta 3 integrin expression. *Eur. J. Nucl. Med. Mol. Imaging 35* (8), 1507−1515. (c) Wu, Y., Zhang, X. Z., Xiong, Z. M., Cheng, Z., Fisher, D. R., Liu, S., Gambhir, S. S., and Chen, X. Y. (2005) microPET imaging of glioma integrin alpha(V)beta(3) expression using Cu-64-labeled tetrameric RGD peptide. *J. Nucl. Med. 46* (10), 1707−1718. (d) Dumont, R. A., Deininger, F., Haubner, R., Maecke, H. R., Weber, W. A., and Fani, M. (2011) Novel Cu-64- and Ga-68-labeled RGD conjugates show improved PET imaging of alpha(v)beta(3) integrin expression and facile radiosynthesis. *J. Nucl. Med. 52* (8), 1276−1284.

(3) (a) Li, Z. B., Cai, W. B., Cao, Q. Z., Chen, K., Wu, Z. H., He, L. N., and Chen, X. Y. (2007) 64Cu-Labeled "Tetrameric and octameric RGD peptides for small-animal PET of Tumor alpha(v)beta(3) integrin expression. *J. Nucl. Med. 48* (7), 1162−1171. (b) Shi, J., Kim, Y.-S., Zhai, S., Liu, Z., Chen, X., and Liu, S. (2009) Improving tumor uptake and pharmacokinetics of Cu-64-labeled cyclic RGD peptide dimers with Gly(3) and PEG(4) linkers. *Bioconjugate Chem. 20* (4), 750−759. (c) Liu, S. (2009) Radiolabeled cyclic RGD peptides as integrin alpha(v)beta(3)-targeted radiotracers: maximizing binding affinity via bivalency. *Bioconjugate Chem. 20* (12), 2199−2213. (d) Chen, X. Y., Liu, S., Hou, Y. P., Tohme, M., Park, R., Bading, J. R., and Conti, P. S. (2004) MicroPET imaging of breast cancer alpha(v)-integrin expression with Cu-64-labeled dimeric RGD peptides. *Mol. Imaging Biol. 6* (5), 350−359.

(4) (a) Rostovtsev, V. V., Green, L. G., Fokin, V. V., and Sharpless, K. B. (2002) A stepwise Huisgen cycloaddition process: Copper(I)-catalyzed regioselective "ligation" of azides and terminal alkynes. *Angew. Chem., Int. Ed. 41* (14), 2596. (b) Kolb, H. C., Finn, M. G., and Sharpless, K. B. (2001) Click chemistry: Diverse chemical function from a few good reactions. *Angew. Chem., Int. Ed. 40* (11), 2004. (c) Meldal, M., and Tornoe, C. W. (2008) Cu-catalyzed azide-alkyne cycloaddition. *Chem. Rev. 108* (8), 2952−3015. (d) Tornoe, C. W., Christensen, C., and Meldal, M. (2002) Peptidotriazoles on solid phase: 1,2,3 -triazoles by regiospecific copper(I)-catalyzed 1,3-dipolar cycloadditions of terminal alkynes to azides. *J. Org. Chem. 67* (9), 3057−3064.

(5) Li, Z. B., Wu, Z., Chen, K., Chin, F. T., and Chen, X. (2007) Click chemistry for F-18-labeling of RGD peptides and microPET Imaging of tumor integrin alpha(v)beta(3) expression. *Bioconjugate Chem. 18* (6), 1987−1994.

(6) Yim, C. B., Boerman, O. C., de Visser, M., de Jong, M., Dechesne, A. C., Rijkers, D. T. S., and Liskamp, R. M. J. (2009) Versatile conjugation of octreotide to dendrimers by cycloaddition ("click") chemistry to yield high-affinity multivalent cyclic peptide dendrimers. *Bioconjugate Chem. 20* (7), 1323−1331.

(7) Ji, S. D., Czerwinski, A., Zhou, Y., Shao, G. Q., Valenzuela, F., Sowinski, P., Chauhan, S., Pennington, M., and Liu, S. (2013) Tc-99m-Galacto-RGD(2): a novel Tc-99m-labeled cyclic RGD peptide dimer useful for tumor imaging. *Mol. Pharmaceutics 10* (9), 3304−3314.

(8) (a) Dijkgraaf, I., Rijnders, A. Y., Soede, A., Dechesne, A. C., van Esse, G. W., Brouwer, A. J., Corstens, F. H. M., Boerman, O. C., Rijkers, D. T. S., and Liskamp, R. M. J. (2007) Synthesis of DOTA-conjugated multivalent cyclic-RGD peptide dendrimers via 1,3-dipolar cycloaddition and their biological evaluation: implications for tumor targeting and tumor imaging purposes. *Org. Biomol. Chem. 5* (6), 935−944. (b) Dijkgraaf, I., Yim, C. B., Franssen, G. M., Schuit, R. C., Luurtsema, G., Liu, S. A., Oyen, W. J. G., and Boerman, O. C. (2011) PET imaging of alpha(v)beta(3) integrin expression in tumours with Ga-68-labelled mono-, di- and tetrameric RGD peptides. *Eur. J. Nucl. Med. Mol. Imaging 38* (1), 128−137.

(9) (a) Aumailley, M., Gurrath, M., Muller, G., Calvete, J., Timpl, R., and Kessler, H. (1991) Arg-Gly-Asp constrained within cyclic pentapeptides - strong and selective inhibitors of cell-adhesion to vitronectin and laminin fragment-P1. *Febs Lett. 291* (1), 50−54. (b) Pfaff, M., Tangemann, K., Muller, B., Gurrath, M., Muller, G., Kessler, H., Timpl, R., and Engel, J. (1994) Selective recognition of cyclic RGD peptides of NMR defined conformation by alpha-II-beta-3, alpha-v-beta-3, and alpha-5-beta-1 integrins. *J. Biol. Chem. 269* (32), 20233−20238.

(10) (a) Haubner, R., Gratias, R., Diefenbach, B., Goodman, S. L., Jonczyk, A., and Kessler, H. (1996) Structural and functional aspects of RGD-containing cyclic pentapeptides as highly potent and selective integrin alpha(v)beta(3) antagonists. *J. Am. Chem. Soc. 118* (32), 7461−7472. (b) Haubner, R., Finsinger, D., and Kessler, H. (1997) Stereoisomeric peptide libraries and peptidomimetics for designing selective inhibitors of the alpha(V)beta(3) integrin for a new cancer therapy. *Angew. Chem., Int. Ed. 36* (13−14), 1375−1389. (c) Gurrath, M., Muller, G., Kessler, H., Aumailley, M., and Timpl, R. (1992) Conformation activity studies of rationally designed potent anti-adhesive RGD peptides. *Eur. J. Biochem. 210* (3), 911−921.

(11) Dai, X. D., Su, Z., and Liu, J. O. (2000) An improved synthesis of a selective alpha(v)beta(3)-integrin antagonist cyclo(-RGDfK-). *Tetrahedron Lett. 41* (33), 6295−6298.

(12) (a) Wang, L. J., Shi, J. Y., Kim, Y. S., Zhai, S. Z., Jia, B., Zhao, H. Y., Liu, Z. F., Wang, F., Chen, X. Y., and Liu, S. (2009) Improving tumor-targeting capability and pharmacokinetics of Tc-99m-labeled cyclic RGD dimers with PEG(4) linkers. *Mol. Pharmaceutics 6* (1), 231−245. (b) Li, Y., Schaffer, P., and Perrin, D. M. (2013) Dual isotope labeling: Conjugation of P-32-oligonucleotides with F-18-aryltrifluoroborate via copper(I) catalyzed cycloaddition. *Bioorg. Med. Chem. Lett. 23* (23), 6313−6316.

(13) (a) Lim, J., and Simanek, E. E. (2012) Triazine dendrimers as drug delivery systems: From synthesis to therapy. *Adv. Drug Delivery Rev. 64* (9), 826−835. (b) Dijkgraaf, I., and Boerman, O. C. (2009) Radionuclide imaging of tumor angiogenesis. *Cancer Biother. Radiopharm. 24* (6), 637−647.

(14) Gavrilyuk, J. I., Wuellner, U., Salahuddin, S., Goswami, R. K., Sinha, S. C., and Barbas, C. F., III (2009) An efficient chemical approach to bispecific antibodies and antibodies of high valency. *Bioorg. Med. Chem. Lett. 19* (14), 3716−3720.

(15) Lim, J., Turkbey, B., Bernardo, M., Bryant, L. H., Garzoni, M., Pavan, G. M., Nakajima, T., Choyke, P. L., Simanek, E. E., and Kobayashi, H. (2012) Gadolinium MRI contrast agents based on triazine dendrimers: relaxivity and in vivo pharmacokinetics. *Bioconjugate Chem. 23* (11), 2291−2299.
(16) Liu, S., Zavalij, P. Y., Lam, Y. F., and Isaacs, L. (2007) Refolding foldamers: Triazene-arylene oligomers that change shape with chemical stimuli. *J. Am. Chem. Soc. 129* (36), 11232−11241.
(17) Chen, X. Y., Park, R., Tohme, M., Shahinian, A. H., Bading, J. R., and Conti, P. S. (2004) MicroPET and autoradiographic imaging of breast cancer alpha(v)-integrin expression using F-18- and Cu-64-labeled RGD peptide. *Bioconjugate Chem. 15* (1), 41−49.
(18) (a) Shi, J. Y., Wang, L. J., Kim, Y. S., Zhai, S. Z., Liu, Z. F., Chen, X. Y., and Liu, S. (2008) Improving tumor uptake and excretion kinetics of Tc-99m-labeled cyclic arginine-glycine-aspartic (RGD) dimers with triglycine linkers. *J. Med. Chem. 51* (24), 7980−7990. (b) Shi, J. Y., Kim, Y. S., Zhai, S. Z., Liu, Z. F., Chen, X. Y., and Liu, S. (2009) Improving tumor uptake and pharmacokinetics of Cu-64-labeled cyclic RGD peptide dimers with Gly(3) and PEG(4) linkers. *Bioconjugate Chem. 20* (4), 750−759.
(19) Wadas, T. J., Wong, E. H., Weisman, G. R., and Anderson, C. J. (2010) Coordinating radiometals of copper, gallium, indium, yttrium, and zirconium for PET and SPECT imaging of disease. *Chem. Rev. 110* (5), 2858−2902.
(20) (a) Eder, M., Loehr, T., Bauder-Wuest, U., Reber, M., Mier, W., Schaefer, M., Haberkorn, U., and Eisenhut, M. (2013) Pharmacokinetic properties of peptidic radiopharmaceuticals: reduced uptake of (EH)(3)-conjugates in important organs. *J. Nucl. Med. 54* (8), 1327−1330. (b) Hosseinimehr, S. J., Tolmachev, V., and Orlova, A. (2012) Liver uptake of radiolabeled targeting proteins and peptides: considerations for targeting peptide conjugate design. *Drug Discovery Today 17* (21−22), 1224−1232. (c) Rogers, B. E., Franano, F. N., Duncan, J. R., Edwards, W. B., Anderson, C. J., Connett, J. M., and Welch, M. J. (1995) Identification of metabolites of 111In-diethylenetriaminepentaacetic acid-monoclonal antibodies and antibody fragments in vivo. *Cancer Res. 55* (23 Suppl), 5714s−5720s. (d) Duncan, J. R., and Welch, M. J. (1993) Intracellular metabolism of indium-111-DTPA-labeled receptor targeted proteins. *J. Nucl. Med. 34* (10), 1728−1738.
(21) Shuhendler, A. J., Prasad, P., Leung, M., Rauth, A. M., DaCosta, R. S., Wu, X. Y., and Novel Solid, A. (2012) Lipid nanoparticle formulation for active targeting to tumor alpha(v)beta(3) integrin receptors reveals cyclic RGD as a double-edged sword. *Advanced Healthcare Materials 1* (5), 600−608.
(22) (a) Yim, C. B., van der Wildt, B., Dijkgraaf, I., Joosten, L., Eek, A., Versluis, C., Rijkers, D. T. S., Boerman, O. C., and Liskamp, R. M. J. (2011) Spacer effects on in vivo properties of DOTA-conjugated dimeric Tyr(3) octreotate peptides, synthesized via a 'Cu(I)-Click' and 'sulfo-Click' ligation method. *J. Labelled Compd. Radiopharm. 54*, S217−S217. (b) Jia, B., Liu, Z., Shi, J., Yu, Z., Yang, Z., Zhao, H., He, Z., Liu, S., and Wang, F. (2008) Linker effects on biological properties of In-111-Labeled DTPA conjugates of a cyclic RGDfK dimer. *Bioconjugate Chem. 19* (1), 201−210. (c) Dijkgraaf, I., Liu, S., Kruijtzer, J. A. W., Soede, A. C., Oyen, W. J. G., Liskamp, R. M. J., Corstens, F. H. M., and Boerman, O. C. (2007) Effects of linker variation on the in vitro and in vivo characteristics of an In-111-labeled RGD peptide. *Nucl. Med. Biol. 34* (1), 29−35.
(23) (a) Wheeler, T. D., Zeng, D., Desai, A. V., Oenal, B., Reichert, D. E., and Kenis, P. J. A. (2010) Microfluidic labeling of biomolecules with radiometals for use in nuclear medicine. *Lab Chip 10* (24), 3387−3396. (b) Zeng, D., Desai, A. V., Ranganathan, D., Wheeler, T. D., Kenis, P. J. A., and Reichert, D. E. (2013) Microfluidic radiolabeling of biomolecules with PET radiometals. *Nucl. Med. Biol. 40* (1), 42−51.
(24) Stroock, A. D., Dertinger, S. K. W., Ajdari, A., Mezic, I., Stone, H. A., and Whitesides, G. M. (2002) Chaotic mixer for microchannels. *Science 295* (5555), 647−651.
(25) Rogers, B. E., McLean, S. F., Kirkman, R. L., Della Manna, D., Bright, S. J., Olsen, C. C., Myracle, A. D., Mayo, M. S., Curiel, D. T., and Buchsbaum, D. J. (1999) In vivo localization of In-111 -DTPA-D-Phe(1)-octreotide to human ovarian tumor xenografts tnduced to express the somatostatin receptor subtype 2 using an adenoviral vector. *Clin. Cancer Res. 5* (2), 383−393.